

Article

The Yinshan Mountains Record over 10,000 Landslides

Jingjing Sun ^{1,2}, Chong Xu ^{2,3,*} , Liye Feng ^{1,2}, Lei Li ⁴, Xuewei Zhang ^{1,2} and Wentao Yang ¹ 

¹ School of Soil and Water Conservation, Beijing Forestry University, Beijing 100083, China; yzijing202108@163.com (J.S.); yang_wentao@bjfu.edu.cn (W.Y.)

² National Institute of Natural Hazards, Ministry of Emergency Management of China, Beijing 100085, China

³ Key Laboratory of Compound and Chained Natural Hazards Dynamics, Ministry of Emergency Management of China, Beijing 100085, China

⁴ Institute of Geology and Geophysics, Chinese Academy of Sciences, Beijing 100029, China

* Correspondence: xc1111111@126.com

Abstract: China boasts a vast expanse of mountainous terrain, characterized by intricate geological conditions and structural features, resulting in frequent geological disasters. Among these, landslides, as prototypical geological hazards, pose significant threats to both lives and property. Consequently, conducting a comprehensive landslide inventory in mountainous regions is imperative for current research. This study concentrates on the Yinshan Mountains, an ancient fault-block mountain range spanning east–west in the central Inner Mongolia Autonomous Region, extending from Langshan Mountains in the west to Damaqun Mountains in the east, with the narrow sense Xiao–Yin Mountains District in between. Employing multi-temporal high-resolution remote sensing images from Google Earth, this study conducted visual interpretation, identifying 10,968 landslides in the Yinshan area, encompassing a total area of 308.94 km². The largest landslide occupies 2.95 km², while the smallest covers 84.47 m². Specifically, the Langshan area comprises 331 landslides with a total area of 11.96 km², the narrow sense Xiao–Yin Mountains include 3393 landslides covering 64.13 km², and the Manhan Mountains, Damaqun Mountains, and adjacent areas account for 7244 landslides over a total area of 232.85 km². This research not only contributes to global landslide cataloging initiatives but also serves as a robust foundation for future geohazard prevention and management efforts.



Citation: Sun, J.; Xu, C.; Feng, L.; Li, L.; Zhang, X.; Yang, W. The Yinshan Mountains Record over 10,000 Landslides. *Data* **2024**, *9*, 31. <https://doi.org/10.3390/data9020031>

Academic Editor: Vladimir Sreckovic

Received: 8 January 2024

Revised: 30 January 2024

Accepted: 6 February 2024

Published: 8 February 2024



Copyright: © 2024 by the authors. Licensee MDPI, Basel, Switzerland. This article is an open access article distributed under the terms and conditions of the Creative Commons Attribution (CC BY) license (<https://creativecommons.org/licenses/by/4.0/>).

Keywords: Yinshan Mountains; landslide inventory; Google Earth; database; 10,968 landslides; human–computer interaction (HCI)

1. Introduction

Landslide is a geological phenomenon in which the slope rock and soil mass slides along the through shear failure surface under the influence of gravity [1]. Many domestic and foreign scholars have conducted extensive research on landslide disasters in various regions around the world, as shown in Table 1. In domestic research, Li et al. [2] undertook an inventory study on large landslides in Baoji, Shaanxi, using existing literature, disaster records, and multi-temporal high-resolution remote sensing images from Google Earth, to conduct an inventory of large landslides (area > 5000 m²) in the study area. Through visual interpretation, an inventory containing 3422 landslides with a total area of 360.7 km² was compiled. In response to the 2022 Luding magnitude 6.8 earthquake, Huang et al. [3] designated the range with an intensity above VII as the research area. A total of 5007 coseismic landslides were interpreted, with a total landslide area of 17.36 km². This landslide list supported a series of subsequent studies. In a foreign study, Edwin L. Harp et al. [4] conducted an inventory of landslides triggered by the 12 January 2010 earthquake in Haiti, and, by comparing pre- and post-earthquake satellite images published by the U.S. Geological Survey, mapped 23,567 landslides triggered by strong shaking, with a total area of landslides of 24.69 km². Hakan Tanyaş et al. [5] conducted a study on landslide events in Papua New Guinea, which identified 10,469 landslides with a total landslide area

of 145 km². Of these, 10,469 landslides (with a total area of 145 km²) were triggered by the mainshock, and 1138 landslides (with a total area of 40 km²) were induced by either aftershocks or succeeding rainfall events between 26 February and 19 March. These research results not only enrich the global landslide database, but also provide an important basis for formulating relevant disaster prevention measures and geological risk assessment [6–12]. Over the years, the study of large-scale landslide disasters in major mountain ranges has been a significant focus in the field of geological science, carrying important scientific, social, and environmental implications. On one hand, human settlement areas are typically located on the peripheries of large mountain ranges. Investigating the distribution and evolutionary mechanisms of landslides through landslide inventories provides a scientific basis for the prevention and management of geological disasters. The early detection of landslide signs, coupled with effective warning and mitigation measures, contributes to reducing the losses caused by disasters and enhancing the safety of residents in mountainous regions. On the other hand, mountainous areas often harbor complex ecosystems, and landslide events may inflict severe damage to these ecosystems. Creating landslide inventory maps facilitates studies on landslide susceptibility, offering a better understanding of the impact of landslides on the ecological environment. In China, particularly in ecologically vulnerable regions, attention should be given to the effects of landslides on vegetation cover and soil erosion, with corresponding measures implemented to protect the ecological environment. However, it is worth noting that, despite significant progress in the field of landslide research, systematic research on landslides in large mountain ranges in China is still relatively insufficient. Therefore, this study aims to compile a landslide inventory for the Yinshan Mountains, to fill the gaps in the related research and to provide a more comprehensive scientific basis for the in-depth understanding and effective prevention and control of mountain landslides.

Table 1. Inventory of typical landslides.

Location	Landslides Number	Landslides Area (km ²)	Source
Baoji, Shaanxi	3422	360.7	[2]
Luding, Sichuan	5007	17.36	[3]
Haiti	23,567	24.69	[4]
The Independent State of Papua New Guinea	10,469	145	[5]

For a long time, the Inner Mongolia Autonomous Region, which is an underdeveloped region in the north of China, has not paid sufficient attention to the problem of geologic hazards, so the relevant research results are relatively limited. However, the geological conditions of the region are complex, the ecological environment is relatively fragile, and historically, geologic disasters have been characterized by a wide range of points [13]. With the advancement of economic construction, geologic disasters occur frequently, posing an increasingly serious threat to the lives and properties of the people of the region, so the problem of geological disasters has now become extremely urgent and cannot be ignored. In order to fill this gap, this paper establishes a cataloging database of landslides in the Yinshan Mountains Range region of China using remote sensing technology, which provides practical help for disaster prevention and mitigation in this region.

2. Study Area

The Yinshan Mountains are located in the central part of the Inner Mongolia Autonomous Region, as shown in Figure 1 [14]. In terms of geomorphology, the Yinshan Mountains rise from the Langshan Mountains and the Wula Mountains in the west, and the central part includes the Xiao-Yin Mountains, in a narrow sense, consisting of the Daqing Mountains and other mountain ranges, and extends to the Manhan Mountains and the Damaqun Mountains in the east. It is geographically important as it is bordered by the Jibei

Mountains in the east and the Helan Mountains in the west. The total area of the mountains is 39,729 km², the total length is about 1000 km, with an average elevation of 1500 to 2000 m, and the main peak is Mt. Huhebashige, located in the Langshan Mountains. The Yinshan Mountains span a considerable distance from east to west, covering regions such as Urad Middle Banner, Guyang County, Wuchuan County, Chahar Right Middle Banner, and Chongli County. Climatically and hydrologically, the Yinshan Mountains are situated in the central Inner Mongolian Plateau, serving as the dividing line between the warm-temperate climate of Inner Mongolia and the temperate climate. Additionally, they play a watershed role between the Pacific outflow system and the central Asian inland drainage [15]. In terms of tectonics, the Yinshan Mountains are located in the western section of the northern edge of the North China Block, the southern part is the Ordos paleo plate, and sandwiched between the two is the Hubao graben system on the northern edge of Ordos [16]. Archean and Proterozoic metamorphic rocks are widely distributed in the Yinshan Mountains [17]. The active fault zones in the area include the Langshan Mountains piedmont fault zone, the Seerteng Mountain piedmont fault zone, the Wula Mountains piedmont fault zone, the Daqing Mountain piedmont fault zone, and the Manhan Mountains piedmont fault zone. According to data from the China Earthquake Networks Center, the Yinshan region has experienced relatively few historical earthquakes, with magnitudes predominantly ranging from 5.0 to 6.9. Earthquakes of magnitude 7 and above have occurred six times in recorded history, with lower magnitude earthquakes being more prevalent in recent years. However, despite the relatively low historical seismic frequency in the Yinshan Mountains, its topographical variations, climatic hydrology, and geological structural characteristics make it a region worthy of in-depth investigation. A comprehensive geological survey and monitoring of the Yinshan Mountains will contribute to a better understanding of the potential geological hazards in the area, providing a scientific basis for future prevention and response efforts.

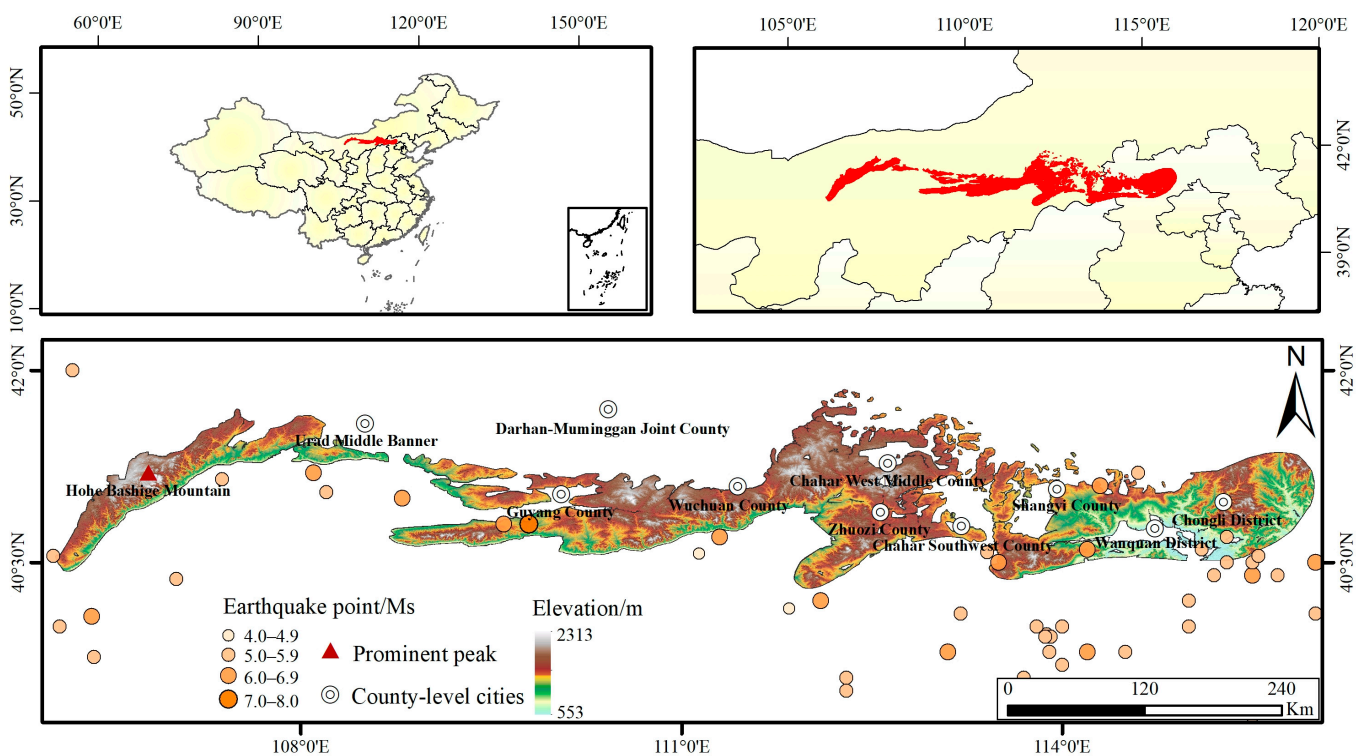


Figure 1. Overview of the study area (vector range source [14,18]).

3. Data and Method

Currently, landslide interpretation mainly uses two mainstream methods: automated landslide extraction and human–computer interaction visual interpretation [19–25]. Automated landslide extraction relies on various algorithms in machine learning to efficiently identify landslides and non-landslide areas by learning the characteristics of sample data to achieve automatic extraction [26]. Its advantages are being fast with a high degree of automation. However, its accuracy will be affected by factors such as remote sensing image type, regional geomorphological characteristics, and landslide type [27]. Therefore, this approach is more suitable for emergency response activities after earthquakes in order to quickly obtain basic information [28]. Visual interpretations for human–computer interactions are still widely used in many current studies [29–31]. Visual interpretation makes full use of human and time resources, and is able to obtain rich and accurate databases [32]. Its strength lies in its robust capability for the objective identification of targets in complex topographic areas, ensuring a more objective and accurate interpretation of results. In this study, human resources and time advantages were maximized for a comprehensive visual interpretation. This approach enabled us to successfully acquire a detailed database of the research area, providing a reliable foundation for subsequent geological hazard studies.

In this study, landslide identification based on images taken from the Google Earth platform was carried out in the Yinshan area. The Google Earth platform includes aerial images and high-resolution satellite images (World View-1, World View-2, and GeoEye-1), with resolutions reaching up to 0.5 m. Making full use of the high-resolution remote sensing images and three-dimensional geomorphological information provided by Google Earth, this study successfully realized the accurate identification of landslides and circled the identified landslides as polygons (Figure 2). To ensure that no potential signs of landslides were overlooked, the Yinshan Mountains were divided into three smaller regions: Langshan District, Xiao–Yin Mountains District in a narrow sense, and the Manhan Mountains, Damaqun Mountains, and surrounding mountainous areas [10,14]. The entirety of the Yinshan Mountains was divided into 19 areas measuring $1^\circ \times 1^\circ$, and we used the Google Earth grid tool to keep the viewing angle constant to conduct refined landslide identification. The recognition process was mainly undertaken by observing various types of features on the images, as shown in Table 2 [33], including the following: (a) topographical features, i.e., whether there are noticeable deformations on the surface; (b) vegetation coverage features, such as the distribution of vegetation and whether its color differs significantly from the surrounding areas; (c) soil characteristics, i.e., whether the soil appears loose, collapsed, or piled up; and (d) river features, as landslides may lead to the obstruction of water bodies or alterations in the direction of water flow. This study comprehensively considers these features to ensure the comprehensive observation and accurate assessment of landslides.

Table 2. Landslide identification criteria.

Identifying Features	Interpretation
Topographical Features	Whether there are noticeable deformations on the surface.
Vegetation Coverage Features	Whether the distribution of vegetation and its color are significantly different from the surrounding area.
Soil Features	Whether the soil appears loose, collapsed, or piled up.
River Features	Whether the body of water is blocked or the direction of flow has changed.

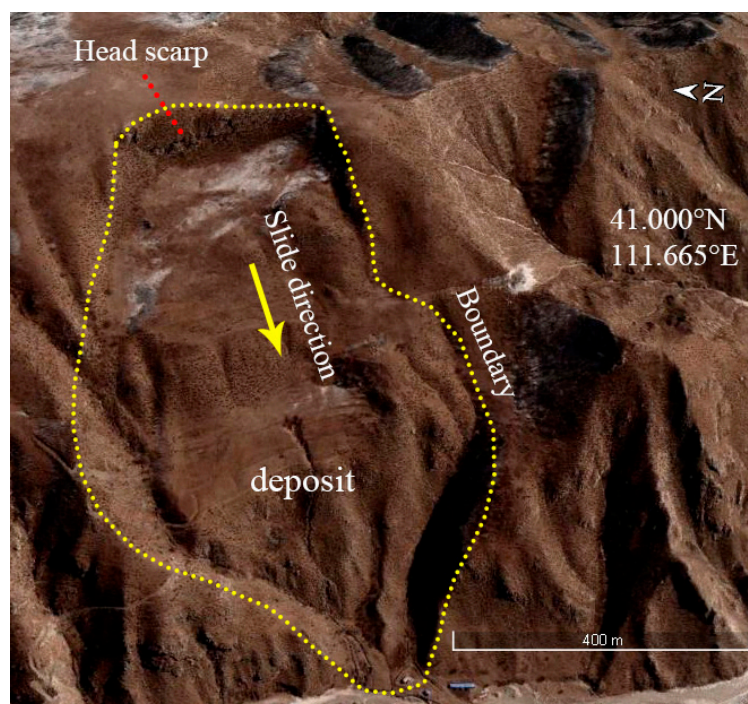


Figure 2. Example of landslide delineation.

4. Results and Analysis

4.1. Inventory of Landslides in the Yinshan Mountains

After 16 months of detailed identification (including cross-validation time) by eight researchers, who all underwent long-term training and were familiar with the geological and geomorphological environment of the study area, the landslide inventory of the Yinshan Mountains was finally completed. Figure 3 illustrates the overall distribution of landslides and the density distribution of landslide sites. Details are shown in Table 3. This study successfully identified and documented 10,968 landslides, covering a total area of 308.94 km² (Figure 3a). The largest landslide encompasses an area of 2.95 km², while the smallest is a mere 84.47 m². There are 377 landslides with an area less than 500 m², with the majority (over 10,000) having an area less than 1 km². This range of landslide sizes reflects the complexity of geological processes and provides comprehensive data support for a deeper understanding of the geological hazard situations in the region.

Table 3. Landslide number and area information.

Mountain Area	Landslides Number	Landslides Area (km ²)	Max. Area (km ²)	Min. Area (m ²)
The Langshan Mountains	331	11.96	0.71	1326
The narrow sense of the Xiao–Yin Mountains	3393	64.13	0.46	84.47
The Manhan Mountains, Damaqun Mountains, and other scattered mountainous areas	7244	232.85	2.95	103
The whole of the Yinshan Mountains	10,968	308.94	2.95	84.47

Figure 3b illustrates the density distribution map of landslides in the Yinshan Mountains. By examining the landslide density map, it is evident that the majority of landslides are concentrated in the central part of the Yinshan Mountains, particularly in the southern branches of the Daqing Mountains and Liangcheng County. The landslide distribution density reaches a high of 4.56 km⁻². Areas with moderate density are primarily located in the central part of the Daqing Mountains, the western part of the Xiao–Yin Mountains,

and the western part of the Damaqun Mountains, among others. This discovery highlights landslide activity in specific geographic areas, providing crucial clues for in-depth research into the geological hazard risks of the region.

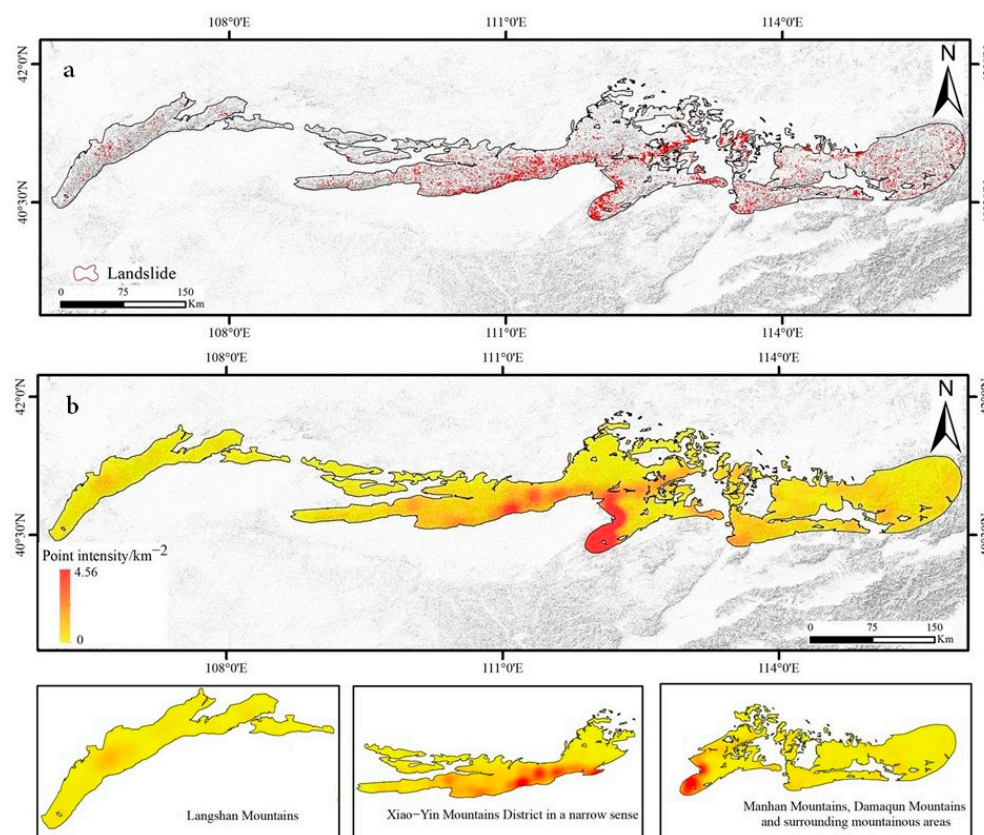


Figure 3. Distribution and density analysis of landslides in the Yinshan Mountains. (a) Landslide distribution. (b) Density distribution of landslide points.

4.2. Detailed Partition Display

To present the landslide distribution in more detail, this study divided the Yinshan Mountains into three regions and illustrated the landslide distribution within each region (Figure 4). In the Langshan Mountains (Figure 4a), landslides are relatively scarce, totaling 331 occurrences with a combined area of 11.96 km². The minimum landslide area is 1326 m², and the maximum is 0.71 km². In the narrow sense of the Xiao-Yin Mountains (Figure 4b), landslides are predominantly concentrated in the southern part of the Daqing Mountains, totaling 3393 occurrences with a combined area of 64.13 km². The minimum landslide area is 84.47 m², and the maximum is 0.46 km². In the Manhan Mountains, Damaqun Mountains, and other scattered mountainous areas (Figure 4c), landslides are most concentrated, accounting for over 65% of the interpreted total. In this region, 7244 landslides were recorded, covering a total area of 232.85 km². The minimum landslide area is 103 m², and the maximum is 2.95 km². This further reveals the variability in landslide distribution across different regions. The high landslide density in this area may be influenced by various geological and topographical factors, necessitating further research to elucidate the specific mechanisms driving landslide activity. Overall, these detailed landslide distribution data provide a crucial foundation for geological hazard risk assessment, early warning system development, and geological hazard prevention and control efforts.

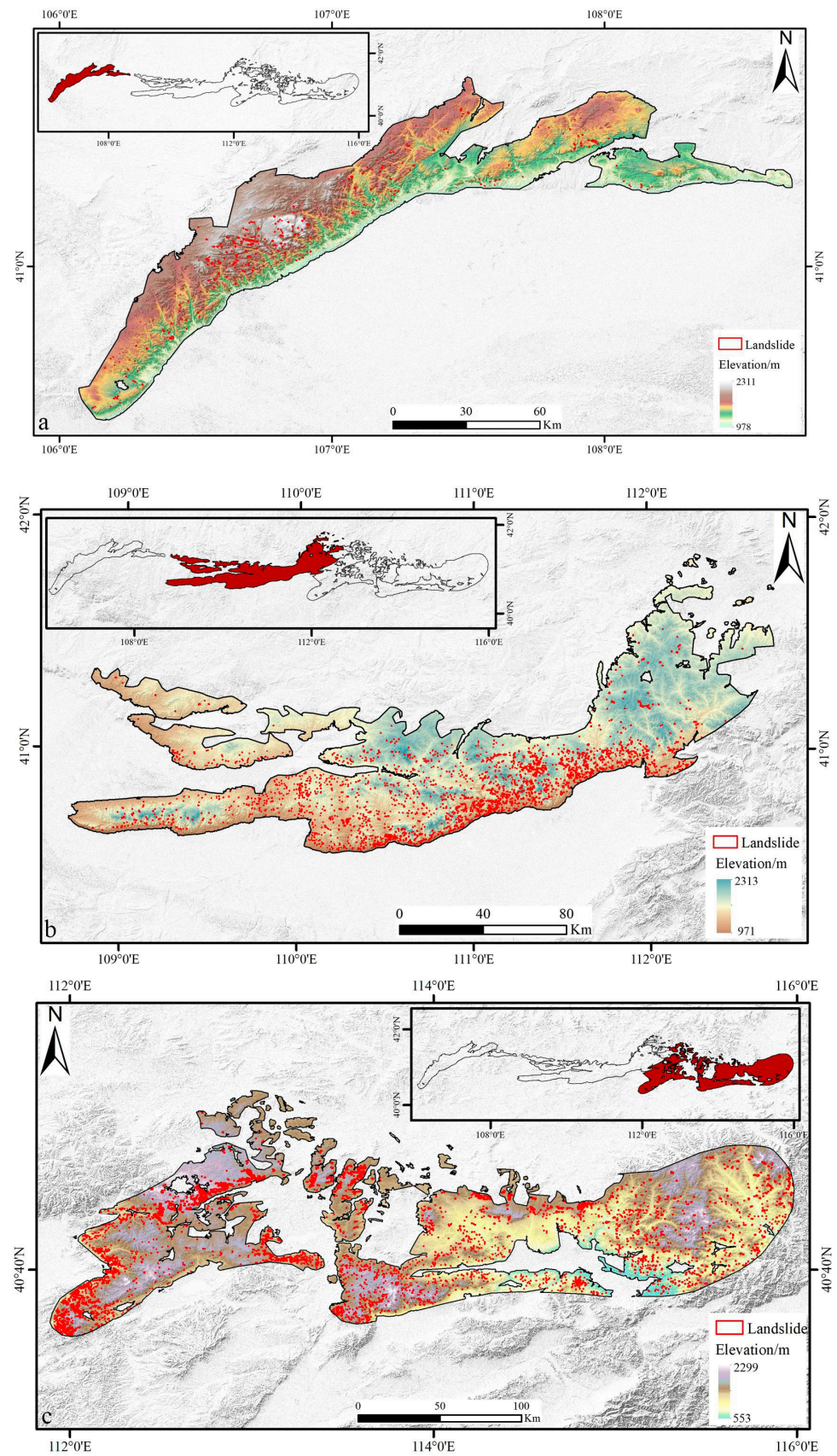


Figure 4. Detailed partition display. (a) Distribution of landslides in Langshan Mountains District. (b) Distribution of landslides in Xiao-Yin Mountains District in a narrow sense. (c) Distribution of landslides in the Manhan Mountains, Damaqun Mountains, and surrounding mountainous areas.

4.3. Typical Landslide Display

In order to show the specific morphology of landslides in the study area in a more detailed and intuitive way, a typical single landslide and a typical group of landslides were selected for display, and Figure 5 shows the location of typical landslides. Figure 6 shows the typical monolithic landslides from west to east in the Yinshan area. The images reveal that the surface layers of these landslides have undergone significant sliding along inclined planes or fault surfaces, displaying distinct features such as the morphology of the landslide mass, the outline of the landslide perimeter, the rear wall of the landslide, and the direction of movement.

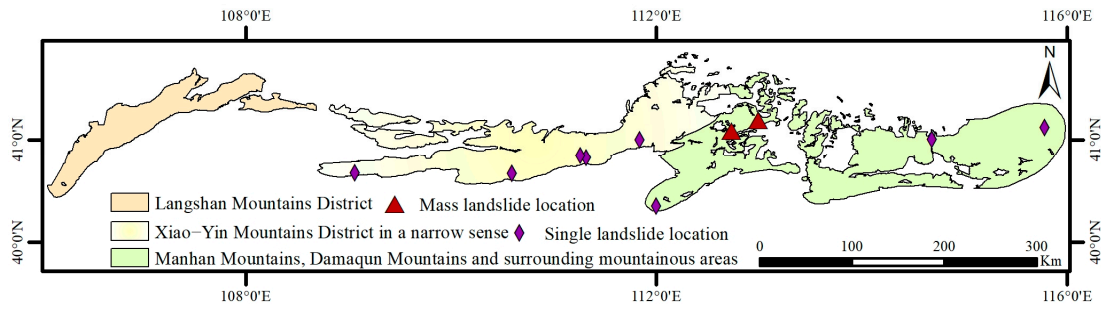


Figure 5. Typical landslide locations.

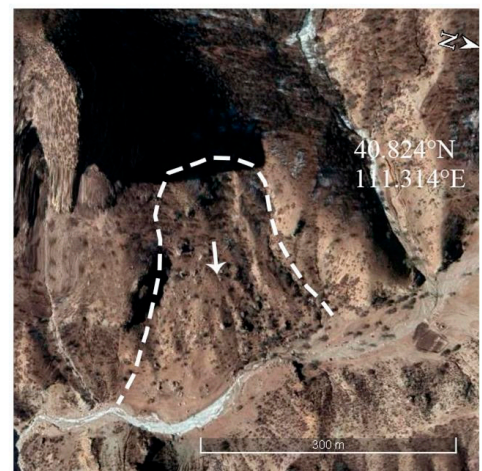
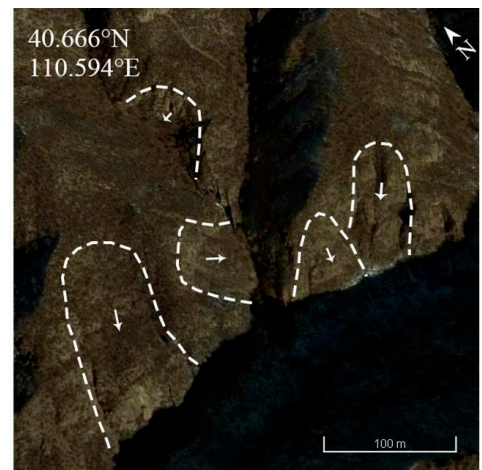
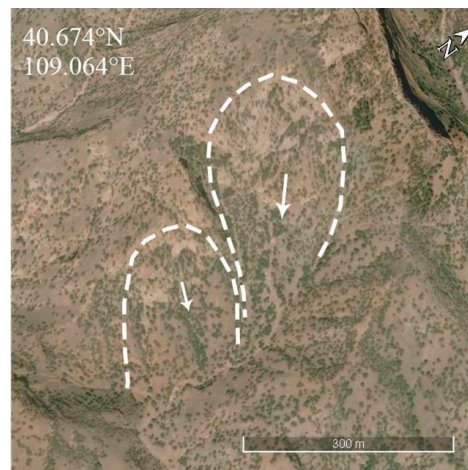


Figure 6. Cont.

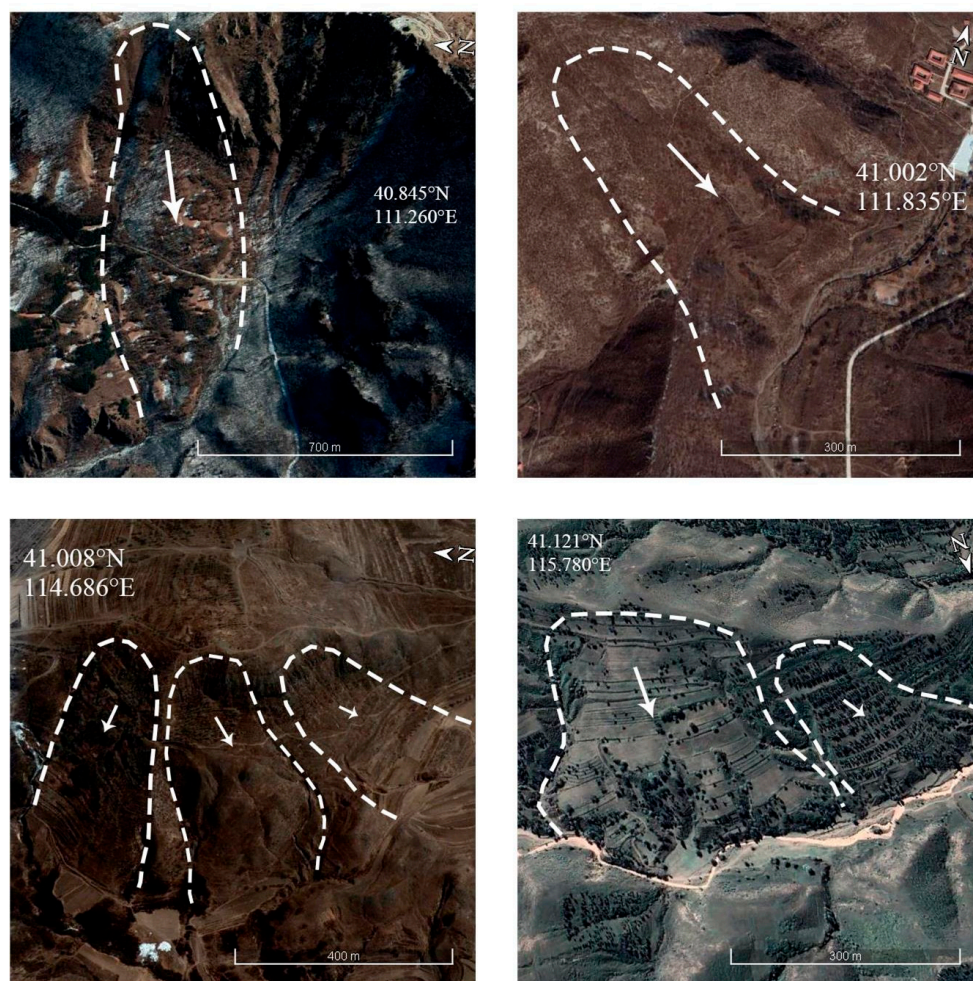


Figure 6. Typical single landslides.

Figure 7 shows two large-scale group landslides in the Yinshan Mountains, located at 41.088° N, 112.733° E and 41.191° N, 112.994° E, respectively. The landslides in this area are relatively concentrated, and the evolution mechanism and process of the landslides are complex, with the formation of sliding surfaces throughout the entire landscape, leading to great geological damage. The evolutionary mechanism of these landslides may involve the interaction of several factors, including topography, geological structure, and climate. By identifying these groups of landslides, the diversity and complexity of Yinshan landslides can be more comprehensively understood.

Identifying landslides through human–computer interaction and visual interpretation can not only capture the overall shape of a single landslide, but also better identify and observe groups of landslides. This is of great significance for understanding the development mechanisms, risk assessments, and possible future geological disasters of Yinshan Mountains landslides, and provides a reliable basis for further geological research and disaster management.

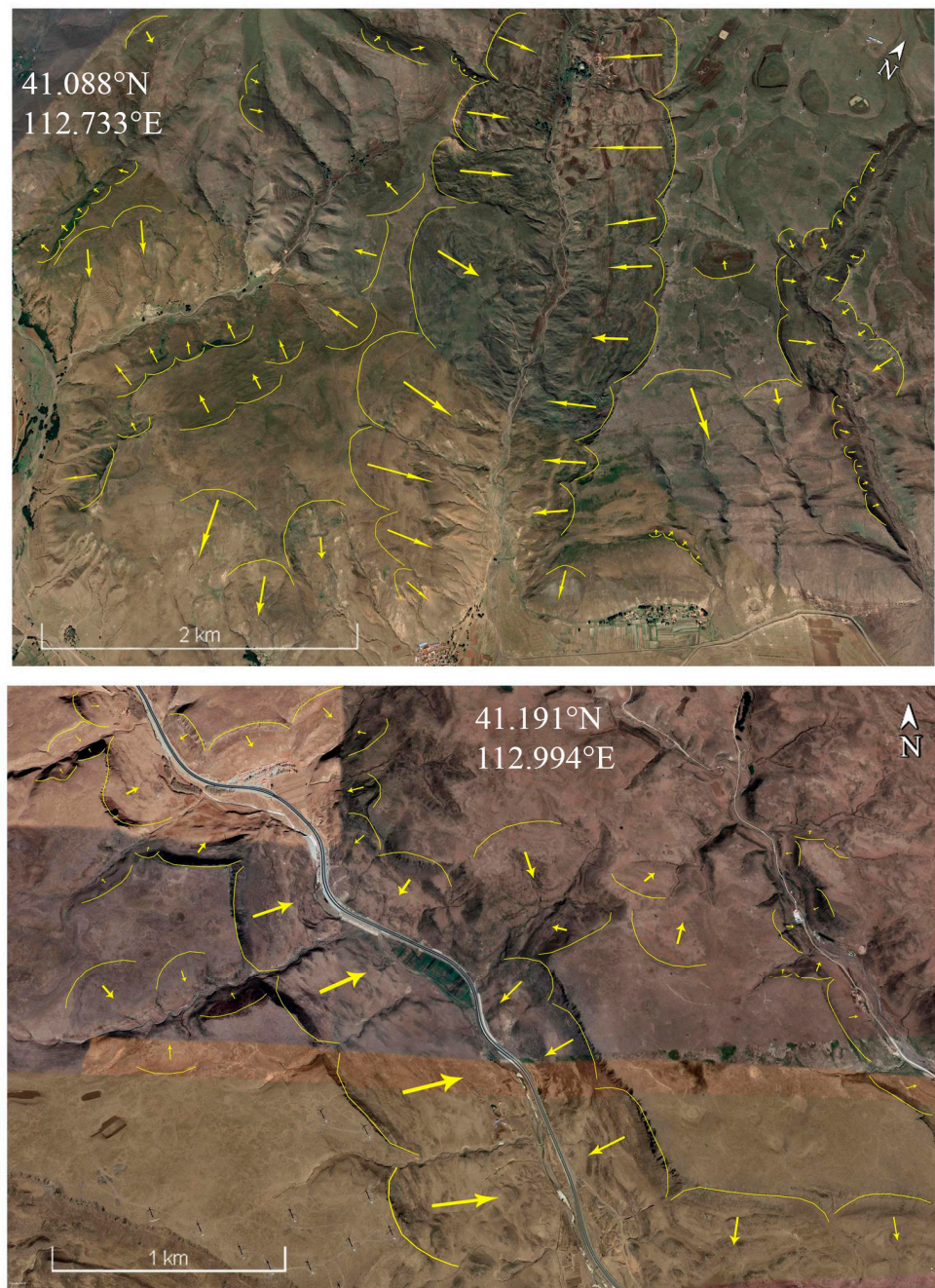


Figure 7. Typical mass landslides.

5. Discussion

At present, many foreign researchers have conducted in-depth research on large-scale mountain landslides, as shown in Table 4. Some outstanding research results have attracted widespread attention. Dawit Asmare et al. [34] conducted a study on the Choke mountain range in northwestern Ethiopia, where he successfully created a landslide inventory map of the range, which covers a total area of 3957.8 km², by combining satellite imagery and field work data. This inventory provides an in-depth look at the mountain's landslide susceptibility. Lulseged Ayalew et al. [35] successfully identified 84.47 landslides around Mount Yahiko in central Japan through the identification of 1:20,000 scale color aerial photos. This study covered a study area of 105 km² and provided strong support for the landslide susceptibility of the area. Pawan Gautam et al. [36] used high-resolution satellite images provided by Google Earth to successfully identify 264 landslides in the

high mountain areas of Nepal. The study area's altitude ranges from 796 m to 5832 m, with a total area of 364 km². Based on this landslide list, he successfully drew a landslide susceptibility map in the high mountain areas of Nepal, which provided a favorable basis for geological hazard research in the region. Mohamed Mastere et al. [37] used remote sensing imagery and aerial photographs to produce a 1:300,000 scale landslide inventory map for the Rif Mountains in northern Morocco through extensive geomorphological analysis. The list contains 4177 landslides with a total area of 1035 km², providing rich data support for geological research in the area. Liesbet Jacobs et al. [38] created the first landslide inventory based on archival information in the Rwenzori Mountains, detailing 48 landslide events and providing an important reference for landslide research in the region. Bastian Morales et al. [39] created a landslide dataset for the Patagonian Andes (42–45° S), containing 10,000 landslides. He pointed out that the lack of geohazard research in the region is mainly due to the low density of available landslide data, which makes it difficult to perform deep learning studies. Hitoshi Saito et al. [40] conducted a study on landslide susceptibility in the Japanese Yatsugatake Mountain Range. The research area, ranging from 150 to 2300 m in elevation, encompassed a total of 194 landslides. By comparing landslide susceptibility with actual landslide occurrences, the study validated a decision tree model and revealed the relationships between landslides, topography and geology. This research unveiled the characteristics of landslides in the region.

Table 4. Inventory of foreign mountain landslides.

Mountain Name	Country	Landslides Number	Landslide Area (km ²)	Purpose/Use	Landslide Data Source	Source
Choke Mountain	Ethiopia	90	/	Mapping landslide susceptibility	Google Earth visual interpretation combined with field investigation	[34]
Kakuda–Yahiko Mountains	Japan	87	5.82	Mapping landslide susceptibility	1:20,000 scale color aerial photographs	[35]
Rif Mountains	Morocco	4177	1065	Enhanced geomorphological hazards and risks to the Rif Mountains	Based on visual interpretation of high-resolution and ultra-high-resolution satellite imagery	[37]
Rwenzori Mountains	Central Africa	48	/	Enriching global landslide inventory	Media reports and laymen accounts	[38]
Central high mountain region of Nepal	Nepal	264	0.599	Mapping landslide susceptibility	Combining aerial photos and satellite images	[36]
Andes Mountains	Patagonia	10,000	/	A machine learning model was built to generate a dataset of terrestrial landslides in the Andes	The trained model in the study area	[39]
Akaishi Mountains	Japan	194	/	Mapping landslide susceptibility	Image difference method	[40]

Although there has been in-depth research on large mountain landslides abroad, there is still a lack of sufficient research in this field domestically. Particularly, there has been no significant progress in creating high-precision inventories of large mountain landslides in China. The absence of detailed landslide inventory data limits our ability to conduct in-depth studies on the spatial distribution, scale, and evolution mechanisms of landslides. Therefore, comprehensive research on large mountain landslides in China needs to be strengthened. This study provides a landslide database in the Yinshan Mountains, but this study also has certain shortcomings and limitations. Firstly, the method used in this study is visual interpretation of human–computer interactions, which lacks field investigations and lacks the ability to verify all the landslides in the list. Secondly, the purpose of splitting the studied area into three small areas in this study was to visually display all

the landslides. There are certain errors in the naming of these small areas with respect to the real mountainous areas. Thirdly, due to the accuracy of remote sensing images relying on Google Earth's accuracy, this research has some shortcomings in the identification of micro landslides. Future studies could focus on establishing a more complete and more accurate inventory of large mountain landslides, utilizing high-precision survey techniques and remote sensing technology to obtain detailed landslide data. This will help researchers to gain a deeper understanding of the spatiotemporal distribution characteristics and evolution mechanisms of landslides, providing a scientific basis for the prevention and management of geological disasters in mountainous regions in China, thus contributing to the social stability and sustainable development of mountainous areas.

6. Conclusions

This study focuses on the generation of foundational data. Through the utilization of high-resolution satellite imagery from the Google Earth platform and employing manual visual interpretation, this study successfully identified 10,968 landslides in the Yinshan Mountains region. The total area of these landslides is 308.94 km², with the largest landslide covering 2.95 km² and the smallest one at 84.47 m². Specifically, the Langshan Mountains region encompasses 331 landslides with a total area of 11.96 km², the narrow sense Xiao–Yin Mountains area contains 3393 landslides totaling 64.13 km², and the Manhan Mountains, Damaqun Mountains, and surrounding areas have a combined total of 7244 landslides, covering 232.85 km². The results indicate that these landslides are mainly concentrated in the central part of the Yinshan Mountains, exhibiting a spatial clustering tendency. The compilation of the landslide inventory for the Yinshan region provides robust support for geological research and environmental management in the area. This inventory not only offers a comprehensive geological database for relevant disciplines but also serves as a scientific basis for formulating rational policies and emergency measures for geological hazard prevention and control. Future research, building upon these findings, can delve deeper into the causal mechanisms and evolutionary patterns of landslides in the Yinshan region, enhancing the accuracy of disaster risk assessments and providing more precise scientific support for the area's sustainable development and ecological preservation.

Author Contributions: C.X. and W.Y. proposed the research concept and provided basic data; L.F., L.L. and X.Z. provided basic data; and J.S. processed the initial data and wrote the manuscript. All authors have read and agreed to the published version of the manuscript.

Funding: This research was supported by the Beijing Science and Technology Plan Project (Z231100003823035) and the National Institute of Natural Hazards, Ministry of Emergency Management of China (2023-JBKY-57).

Institutional Review Board Statement: Not applicable.

Informed Consent Statement: Not applicable.

Data Availability Statement: The datasets used and/or analyzed during the current study are available from the corresponding author on reasonable request.

Acknowledgments: We are grateful to the anonymous reviewers for their constructive comments and suggestions that improved the quality of the manuscript.

Conflicts of Interest: The authors declare no conflicts of interest.

References

1. Xu, Q. Deformation and failure behavior and intrinsic mechanism of landslides. *J. Eng. Geol.* **2012**, *20*, 145–151.
2. Li, L.; Xu, C.; Yang, Z.; Zhang, Z.; Lv, M. An Inventory of Large-Scale Landslides in Baoji City, Shaanxi Province, China. *Data* **2022**, *7*, 114. [\[CrossRef\]](#)
3. Huang, Y.; Xie, C.; Li, T.; Xu, C.; He, X.; Shao, X.; Xu, X.; Zhan, T.; Chen, Z. An open-accessed inventory of landslides triggered by the MS 6.8 Luding earthquake, China on September 5, 2022. *Earthq. Res. Adv.* **2023**, *3*, 100181. [\[CrossRef\]](#)
4. Harp, E.L.; Jibson, R.W.; Schmitt, R.G. Map of landslides triggered by the January 12, 2010, Haiti earthquake. *US Geol. Surv. Sci. Invest. Map.* **2016**, 3353, 15.

5. Tanyaş, H.; Hill, K.; Mahoney, L.; Fadel, I.; Lombardo, L. The world's second-largest, recorded landslide event: Lessons learnt from the landslides triggered during and after the 2018 Mw 7.5 Papua New Guinea earthquake. *Eng. Geol.* **2022**, *297*, 103504. [[CrossRef](#)]
6. Kavzoglu, T.; Colkesen, I.; Sahin, E.K. Machine learning techniques in landslide susceptibility mapping: A survey and a case study. In *Landslides: Theory, Practice and Modelling*; Springer: Cham, Switzerland, 2019; pp. 283–301.
7. Van Den Eeckhaut, M.; Hervás, J.; Jaedicke, C.; Malet, J.-P.; Montanarella, L.; Nadim, F. Statistical modelling of Europe-wide landslide susceptibility using limited landslide inventory data. *Landslides* **2012**, *9*, 357–369. [[CrossRef](#)]
8. Casagli, N.; Catani, F.; Puglisi, C.; Delmonaco, G.; Ermini, L.; Margottini, C. An inventory-based approach to landslide susceptibility assessment and its application to the Virginio River Basin, Italy. *Environ. Eng. Geosci.* **2004**, *10*, 203–216. [[CrossRef](#)]
9. Hervás, J.; Bobrowsky, P. Mapping: Inventories, susceptibility, hazard and risk. In *Landslides—Disaster Risk Reduction*; Springer: Berlin/Heidelberg, Germany, 2009; pp. 321–349.
10. Van Den Eeckhaut, M.; Reichenbach, P.; Guzzetti, F.; Rossi, M.; Poesen, J. Combined landslide inventory and susceptibility assessment based on different mapping units: An example from the Flemish Ardennes, Belgium. *Nat. Hazards Earth Syst. Sci.* **2009**, *9*, 507–521. [[CrossRef](#)]
11. Zêzere, J.; Pereira, S.; Melo, R.; Oliveira, S.; Garcia, R.A. Mapping landslide susceptibility using data-driven methods. *Sci Total Environ.* **2017**, *589*, 250–267. [[CrossRef](#)]
12. Van, C.; Castellanos, E.; Kuriakose, S. Spatial data for landslide susceptibility, hazard, and vulnerability assessment: An overview. *Eng. Geol.* **2008**, *102*, 112–131.
13. Bao, S.; Bao, W.; Bao, Y. Research on Inner Mongolia geological disaster information system based on GIS. In *Information Technology in Risk Analysis and Crisis Response, Proceedings of the Sixth Annual Meeting of the Risk Analysis Professional Committee of the China Disaster Prevention Association*; Atlantis Press: Amsterdam, The Netherlands, 2014.
14. Nan, X.; Li, A.; Deng, W. Data Set of “Digital Mountain Map of China”. A Big Earth Data Platform for Three Poles. 2022. Available online: <https://data.tpdc.ac.cn/en/data/efa1dc3f-5f2d-4e60-8bf7-3ea4c6ec1929/> (accessed on 5 January 2024).
15. Zhang, C.; Xu, J.; Wu, G.; Gong, X.; Yang, M.; Zhao, Z.; Li, M. Overview of plants resources in Yinshan Mountain range and Its achievements. *Mod. Chin. Med.* **2018**, *20*, 253–261.
16. Wang, Q.; Teng, J.; Wang, G.; Xu, Y. The region gravity and magnetic anomaly fields and the deep structure in Yinshan mountains of Inner Mongolia Chinese. *J. Geophys.* **2005**, *48*, 314–320. (In Chinese)
17. Hou, J.; Zhuang, X.; Liu, Y. Analysis on relationship between geological hazards and geological environment in Inner Mongolia autonomous region. *J. Catastrophol.* **2013**, *28*, 66–72.
18. Deng, W.; Li, A.; Nan, X.; Chen, Y.; Liao, K. *China Digital Mountain Map*; China Map Publishing House: Beijing, China, 2015.
19. Dai, F.; Xu, C.; Yao, X.; Xu, L.; Tu, X.; Gong, Q. Spatial distribution of landslides triggered by the 2008 Ms 8.0 Wenchuan earthquake, China. *China J. Asian Earth Sci.* **2011**, *40*, 883–895. [[CrossRef](#)]
20. Fiorucci, F.; Ardizzone, F.; Mondini, A.C.; Viero, A.; Guzzetti, F. Visual interpretation of stereoscopic NDVI satellite images to map rainfall-induced landslides. *Landslides* **2019**, *16*, 165–174. [[CrossRef](#)]
21. Huang, F.; Tao, S.; Chang, Z.; Huang, J.; Fan, X.; Jiang, S.-H.; Li, W. Efficient and automatic extraction of slope units based on multi-scale segmentation method for landslide assessments. *Landslides* **2021**, *18*, 3715–3731. [[CrossRef](#)]
22. Liu, P.; Wei, Y.; Wang, Q.; Xie, J.; Chen, Y.; Li, Z.; Zhou, H. A research on landslides automatic extraction model based on the improved mask R-CNN. *ISPRS Int. J. Geo-Inf.* **2021**, *10*, 168. [[CrossRef](#)]
23. Fiorucci, F.; Cardinali, M.; Carlà, R.; Rossi, M.; Mondini, A.; Santurri, L.; Ardizzone, F.; Guzzetti, F. Seasonal landslide mapping and estimation of landslide mobilization rates using aerial and satellite images. *Geomorphology* **2011**, *129*, 59–70. [[CrossRef](#)]
24. Othman, A.A.; Gloaguen, R. Automatic extraction and size distribution of landslides in Kurdistan region, NE Iraq. *Remote Sens.* **2013**, *5*, 2389–2410. [[CrossRef](#)]
25. Yang, S.; Li, Y.; Feng, G.; Zhang, L. A method aimed at automatic landslide extraction based on background values of satellite imagery. *Int. J. Remote Sens.* **2014**, *35*, 2247–2266. [[CrossRef](#)]
26. Liu, P.; Wei, Y.; Wang, Q.; Chen, Y.; Xie, J. Research on post-earthquake landslide extraction algorithm based on improved U-Net model. *Remote Sens.* **2020**, *12*, 894. [[CrossRef](#)]
27. Hernandez, N.; Pastrana, A.; Garcia, L.; de Leon, J.; Alvarez, A.; Morales, L.; Nemiga, X.; Posadas, G. Co-seismic landslide detection after M 7.4 earthquake on June 23, 2020, in Oaxaca, Mexico, based on rapid mapping method using high and medium resolution synthetic aperture radar (SAR) images. *Landslides* **2021**, *18*, 3833–3844. [[CrossRef](#)]
28. Sun, J.; Shao, X.; Feng, L.; Xu, C.; Huang, Y.; Yang, W. An essential update on the inventory of landslides triggered by the Jiuzhaigou Mw6. 5 earthquake in China on 8 August 2017, with their spatial distribution analyses. *Heliyon* **2024**, *10*, e24787. [[CrossRef](#)]
29. Pawluszek, K. Landslide features identification and morphology investigation using high-resolution DEM derivatives. *Nat. Hazards* **2019**, *96*, 311–330. [[CrossRef](#)]
30. Santangelo, M.; Gioia, D.; Cardinali, M.; Guzzetti, F.; Schiattarella, M. Landslide inventory map of the upper Sinni River valley, Southern Italy. *J. Maps.* **2015**, *11*, 444–453. [[CrossRef](#)]

31. Wati, S.; Hastuti, T.; Widjojo, S.; Pinem, F. Landslide susceptibility mapping with heuristic approach in mountainous area: A case study in Tawangmangu sub district Central Java, Indonesia. *Int. Arch. Photogramm. Remote Sens. Spat. Inf. Sci.* **2010**, *38*. Available online: https://www.isprs.org/PROCEEDINGS/XXXVIII/part8/pdf/W01P04_20100312174755.pdf (accessed on 5 January 2024).
32. Huang, Y.; Xu, C.; Li, L.; He, X.; Cheng, J.; Xu, X.; Li, J.; Zhang, X. Inventory and spatial distribution of ancient Landslides in Hualong County, China. *Land* **2022**, *12*, 136. [[CrossRef](#)]
33. Shao, X.; Xu, C.; Li, L.; Yang, Z.; Yao, X.; Shao, B.; Liang, C.; Xue, Z.; Xu, X. Spatial analysis and hazard assessment of Large-scale ancient landslides around the reservoir area of Wudongde Hydropower Station, China. *Nat. Hazards* **2023**. Available online: <https://www.researchsquare.com/article/rs-2805236/v1> (accessed on 5 January 2024).
34. Asmare, D. Application and validation of AHP and FR methods for landslide susceptibility mapping around choke mountain, northwestern ethiopia. *Sci. Afr.* **2023**, *19*, e01470. [[CrossRef](#)]
35. Ayalew, L.; Yamagishi, H. The application of GIS-based logistic regression for landslide susceptibility mapping in the Kakuda-Yahiko Mountains, Central Japan. *Geomorphology* **2005**, *65*, 15–31. [[CrossRef](#)]
36. Gautam, P.; Kubota, T.; Sapkota, L.M.; Shinohara, Y. Landslide susceptibility mapping with GIS in high mountain area of Nepal: A comparison of four methods. *Environ. Earth Sci.* **2021**, *80*, 359. [[CrossRef](#)]
37. Mastere, M.; El Fellah, B.; Maquaire, O. Landslides inventory map as a first step for hazard and risk assessment: Rif mountains, Morocco. *Bull. De L'Inst. Sci. Rabat Sect. Sci. De La Terre* **2020**, *42*, 49–62.
38. Jacobs, L.; Dewitte, O.; Poesen, J.; Delvaux, D.; Thiery, W.; Kervyn, M. The Rwenzori Mountains, a landslide-prone region? *Landslides* **2016**, *13*, 519–536. [[CrossRef](#)]
39. Morales, B.; Garcia-Pedrero, A.; Lizama, E.; Lillo-Saavedra, M.; Gonzalo-Martín, C.; Chen, N.; Somos-Valenzuela, M. Patagonian Andes Landslides Inventory: The deep learning's way to their automatic detection. *Remote Sens.* **2022**, *14*, 4622. [[CrossRef](#)]
40. Saito, H.; Nakayama, D.; Matsuyama, H. Comparison of landslide susceptibility based on a decision-tree model and actual landslide occurrence: The Akaishi Mountains, Japan. *Geomorphology* **2009**, *109*, 108–121. [[CrossRef](#)]

Disclaimer/Publisher's Note: The statements, opinions and data contained in all publications are solely those of the individual author(s) and contributor(s) and not of MDPI and/or the editor(s). MDPI and/or the editor(s) disclaim responsibility for any injury to people or property resulting from any ideas, methods, instructions or products referred to in the content.